SMOS and SMAP Brightness Temperature Assimilation Over the Murrumbidgee Basin

Dominik Rains, Gabrielle J. M. De Lannoy, Hans Lievens, Jeffrey P. Walker, and Niko E. C. Verhoest

Abstract—**With the launch of the Soil Moisture and Ocean Salinity (SMOS) mission in 2009 and the Soil Moisture Active-Passive (SMAP) mission in 2015, a wealth of L-band brightness temperature (Tb) observations has become available. In this letter, SMOS and SMAP Tbs are assimilated separately into the Community Land Model over the Murrumbidgee basin in south-east Australia from April 2015 to August 2017. To overcome the seasonal Tb observation-minus-forecast biases, Tb anomalies from the seasonal climatology are assimilated. The use of climatologies derived from either SMOS or SMAP observations using either 2 years or 7 years of data yields nearly identical results, highlighting the limited sensitivity to the climatology computation and their interchangeability. The temporal correlation between soil moisture data assimilation results and *in situ* observations is slightly improved for top-layer soil moisture (+0.04) and for root-zone soil moisture (+0.05). The soil moisture anomaly correlation improves moderately for the top-layer soil moisture (+0.15), with a smaller positive impact on the root zone (+0.05).**

Index Terms—**Data assimilation, hydrology, remote sensing, soil moisture.**

I. Introduction

SURFACE soil moisture plays an important role in the global energy and water cycle. It controls the extent to which the incoming solar radiation contributes either to the sensible heat flux, by absorption through the Earth's surface in dry conditions, or to the latent heat flux, by absorption through the soil water [1]. Applications, such as drought and flood monitoring, or studies related to land–atmosphere interactions, can benefit from the availability of accurate soil moisture information. From space, soil moisture can, for example, be derived from the naturally emitted radiance in the microwave spectrum [2]. Therefore, the Soil Moisture and Ocean Salinity (SMOS) mission [3] was launched in November 2009 by the European Space Agency, measuring L-band brightness temperatures (Tb) at multiple angles and at a spatial resolution of 42 km and with an expected accuracy of about 4 K. In January 2015, the Soil Moisture Active-Passive (SMAP) mission [4] was also launched carrying a radiometer to measure the Tb at the L-band with a similar spatial resolution, but with a conically scanning antenna with a single incidence angle of 40° and a higher expected accuracy of 1.3 K. Observations at longer wavelengths, such as L-band, are considered to be optimal, since vegetation has less of a masking effect when compared with other frequencies [2]. Soil moisture retrievals from such data are restricted to the satellite overpass time and the observed soil depth, roughly the top 5 cm. Integrating these retrievals into a land surface model through data assimilation, therefore, has some distinctive advantages. First, the observed soil layers can be updated with information from the soil moisture retrieval, with the model being able to translate the changes in the surface soil moisture to deeper unobserved layers. Alternatively, the deeper layers can be updated directly by making use of the covariance between the observed and unobserved layers [5]. Second, the model can be run at the desired temporal resolution, and thus propagate the observational information through time. The soil moisture retrieval algorithm depends on static and dynamic ancillary data with the latter often provided by a model. Retrieval errors are thus directly linked to errors in these ancillary data. In a data assimilation system that uses its own model and ancillary data, it can therefore be advantageous to directly assimilate the Tb data, allowing for a consistent use of information in the forward Tb simulations and to avoid cross-correlated errors [6].

In this letter, either SMAP (v3.080 [7]) or SMOS (v620) H-polarized Tb observations at a single 40° incidence angle are assimilated into the Community Land Model (CLM) over the Murrumbidgee basin in Australia. The study site was chosen for the availability of a relatively dense *in situ* measurement network and the lack of radio-frequency interference (RFI). To overcome Tb observation-minus-forecast biases, differences between the observation and forecast climatologies are removed as in [6], [8], and [9]. Updates to the model are computed by contrasting unbiased (by design) forecast TB anomalies and observation Tb anomalies, serving the same purpose as assimilating the absolute TBs but with the former being already bias-corrected. This letter differs from earlier TB assimilation studies in the exact calculation of: 1) the climatologies and 2) the anomaly Tb observation-minus-forecasts in the assimilation system. Two experiments assimilate these Tb anomalies from either SMOS or SMAP, after the removal of a 7-year SMOS Tb

Manuscript received May 16, 2018; revised June 26, 2018; accepted July 9, 2018. Date of publication August 2, 2018; date of current version November 5, 2018. This work was supported by the Belgian Science Policy Office in the framework of the STEREO III Programme HYDRAS + Project under Grant SR/00/302. *(Corresponding author: Dominik Rains.)*

D. Rains, H. Lievens, and N. E. C. Verhoest are with the Laboratory of Hydrology and Water Management, Ghent University, 9000 Gent, Belgium (e-mail: dominik.rains@ugent.be).

G. J. M. De Lannoy is with the Department of Earth and Environmental Sciences, Katholieke Universiteit Leuven, 3000 Leuven, Belgium.

J. P. Walker is with the Department of Civil Engineering, Monash University, Clayton, VIC 3800, Australia.

Digital Object Identifier 10.1109/LGRS.2018.2855188

climatology (as in [6] and [8]). Four other experiments are carried out using Tb anomalies obtained after removing 2-year climatologies: one using SMOS and one using SMAP data with their corresponding climatology, and two experiments using the climatology of the other sensor. This letter demonstrates the interchangeability of the Tb climatologies obtained from different, but similar, L-band missions. The similarity in soil moisture improvements for all data assimilation experiments will highlight the synergy between the SMOS and the SMAP mission and the general potential to use an existing (long-term) climatology from established mission as a substitute for a pending climatology of a very new mission. In addition, it will be shown that a consistent improvement in soil moisture can be obtained when calculating anomalies from a climatology-based on a shorter time period. This is, for example, relevant in the areas where a historical sensor failed to collect data (e.g., SMOS data contamination due to RFI), while newer sensors (e.g., SMAP) may facilitate measurements that could be assimilated. The model and assimilation system setup is based on [10] and only the most important aspects are described below.

II. Assimilation System

A. Community Land Model

The CLM is the land surface component of the Community Earth System Model [11] and simulates subsurface soil water within 10 soil layers. For this study, plant functional types (PFTs) are based on the Moderate Resolution Imaging Spectroradiometer (MODIS) MCD12Q1, version 5 land cover product, and reclassified to be compatible with the CLM. Climatological monthly leaf area index for each PFT is computed from the MODIS 8-daily MCD15A3H (version 6) LAI product. The model is run at 0.25° spatial resolution.

B. ERA-Interim Atmospheric Forcing

CLM is run in the off-line mode using atmospheric forcings derived from the ERA-Interim reanalysis [12], with the variables 2-m air temperature, 2-m pressure, short-wave incoming radiation, and total precipitation directly available. Specific humidity is computed from the 2-m dew point temperature and 2-m air temperature, and 2-m wind speed is derived from the wind speed components in the lateral and longitudinal directions. The data were bilinearly interpolated to the model resolution and then temporally interpolated from 3-h data to the 30-min model time step at runtime.

C. Ensemble Member Generation

In order to account for the model uncertainty, CLM is run with 32 ensemble members [10]. Spatially correlated perturbations (correlation length $= 1.25°$) are added to air temperature, shortwave radiation, and precipitation. Shortwave radiation is perturbed with multiplicative noise with a standard deviation of 0.3, whereas for temperature additive noise with a standard deviation of 2.5 K is applied. Precipitation is perturbed with multiplicative log-normal noise with a standard deviation of 0.5. Soil fractions are perturbed once at the model startup with spatially correlated multiplicative noise with a standard deviation of 10% for clay and sand for the top two soil layers. With the increasing layer depth, the multiplicative factor is reduced by using the inverse relationship between the thickness of each layer and the summed soil layer thickness of the two top layers. CLM derives hydraulic properties based on soil texture, resulting in each ensemble member having slightly modified model physics.

D. Forward Tb Simulations

Forward Tb simulations are computed with the Community Microwave Emission Model (CMEM, v5.1 [13]) on the basis of the open-loop (OL) ensemble member output. SMOS and SMAP have an overpass time at approximately 6 A.M. and 6 P.M. local time. Forward simulations are thus computed at 8:00 UTC on the same day and at 20:00 UTC on the previous day, accounting for a time shift of -10 h for the study area. The CMEM setup for this study is identical to the one described in more detail in [10] with the exception of here not computing the atmospheric contribution. The vegetation-dependent parameters are taken from the European Space Agency operational L2 parameter set. A calibration of the parameters was not undertaken to preserve the original sensitivity of the forward simulations toward soil moisture [14]. The forecast Tb anomalies required together with the observation anomalies for computing the soil moisture updates are obtained by removing a seasonally varying Tb forecast climatology. These anomalies are by design unbiased, and mitigating a bias by calibrating the CMEM is therefore not necessary. The forecast climatology is computed using a 31-day moving window averaging all simulations across the same years used for the computation of the observation climatologies, as described below.

E. Tb Observations

For the SMOS Tb observations, contributions from galactic noise as well as the atmosphere are removed to make both the SMOS and SMAP Level 1 Tb observation data sets comparable [15]. Since SMOS Tb observations are available at multiple angles, observations within a 2.5° bin around 40° incidence angle are averaged, which should slightly reduce the uncertainty. For SMAP, forward-looking and aft-looking acquisitions are averaged. Both the data sets are provided on the 36-km Equal-Area Scalable Earth Grid version 2. For the computation of the SMOS and SMAP Tb observation anomaly time series, various SMOS- and SMAP-based climatologies are calculated, always using a 31-day moving window and averaging all observations within that window across the years, again for morning and afternoon overpasses separately. SMOS and SMAP Tb anomalies are then obtained by removing the climatology from the observation time series. The cumulative distribution functions (cdfs) of the observation and forecast anomaly time series are matched at the corresponding 6 A.M. and 6 P.M. overpass times, mainly to reconcile the differences in the variance (and possible higher moments) between the forecast and the observation Tb anomalies (the means of both the observation and model anomalies are nearly zero by design). In this process, special care is taken to ensure that the SMOS ascending (resp. descending) node corresponds to the SMAP descending (resp. ascending) node and to the 6 A.M. (resp. 6 P.M.) forecasts. Three different Tb observation climatologies were computed for each overpass time: 1) a 7-year SMOS Tb climatology; 2) a 2-year SMOS Tb climatology; and 3) a 2-year SMAP Tb climatology. The Tb observation errors are rescaled at each time step using the ratio between the temporal standard deviation of the observation anomalies prior to and after the cdf-matching step. The unscaled observation error variance was defined as 25 K^2 for SMOS (16 K^2 representativeness error + 9 K^2 radiometric error variance) and 17.64 K^2 for SMAP (16 K^2 + 1.69 K^2).

F. Local Ensemble Transform Kalman Filter

The local ensemble transform Kalman filter [16] is an implementation of the ensemble Kalman square-root filter. To reconcile biases between the Tb forecasts and the observations, the respective Tb climatologies are removed from the Tb innovation term, by first calculating anomalies as discussed above. The top six CLM layers are updated corresponding to a depth of 50 cm. Deeper layers are not updated to prevent large root zone updates from having a cascading effect on all the above layers, also due to the increasing layer thickness with depth. It can also be argued that making use of surface observations to update very deep layers is questionable, and so, these are updated through model physics only. At a given grid cell, besides using central observation, surrounding observations are also considered. The observation variance of these neighboring observations is thereby increased with their distance from the grid cell to be updated. This is achieved by multiplying the respective observation variances with a distant-dependent factor computed with the Gaspari–Cohn function [17]. The maximum distance at which observations are considered at all is defined at 100 km. This to some extent mimics the spatial footprint of the satellite observations, which is larger than the spatial resolution at which the data are provided. After each analysis step, a postinflation factor is applied to force the ensemble spread of the 32 ensemble members to approximately the same as before the analysis. This, together with the soil texture perturbations, prevents ensemble collapse especially during dry periods.

III. Results and Validation

An ensemble OL simulation is performed as a reference without any data assimilation. The two assimilation experiments using the long-term SMOS Tb climatology (from July 2010 to June 2017) are referred to herein as SMOSDA and SMAPDA, while the experiments using a 2-year Tb climatology (from July 2015 to June 2017) specific for the assimilated data are referred to as SMOSDA.s and SMAPDA.s, when using their own respective climatology, or SMOSDA.x, when assimilating SMOS Tb using the 2-year SMAP-based climatology, and SMAPDA.x, when assimilating SMAP Tb using the 2-year SMOS-based climatology, i.e., x, for cross-climatologies. For all the experiments, the assimilation period is from

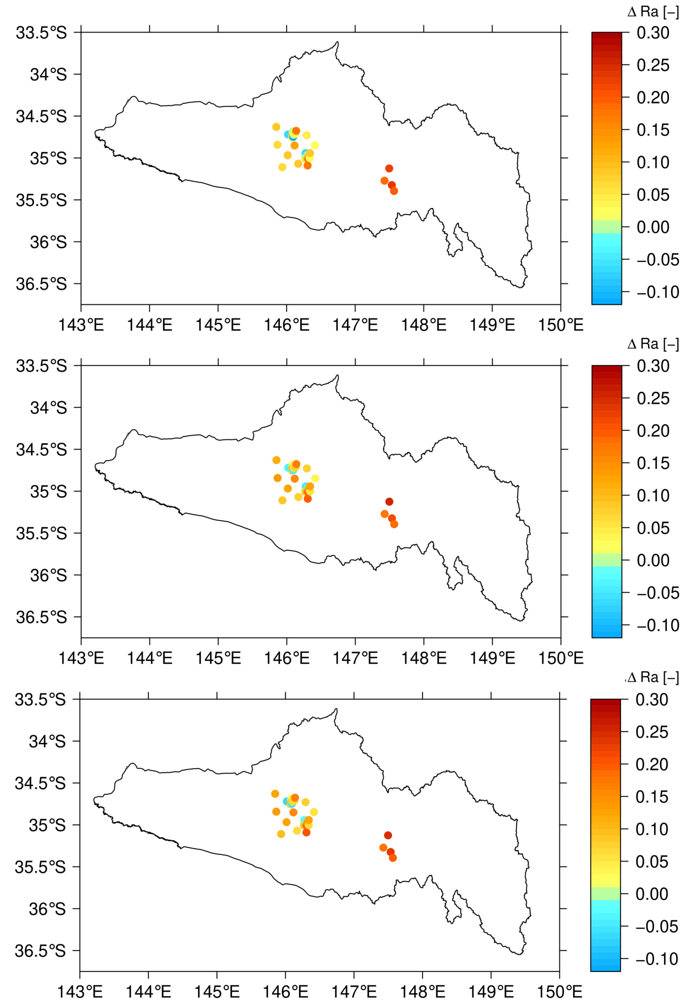

Fig. 1. Impact on Ra for surface soil moisture anomalies for the experiments (Top) SMAPDA, (Middle) SMAPDA.s, and (Bottom) SMAPDA.x.

April 2015 to August 2017. The validation of the 30-min (incl. forecast and analysis) results is performed against *in situ* soil moisture measurements from the OzNet network [18] within the Murrumbidgee catchment, which is located in south-eastern Australia. The catchment changes from low-lying semiarid plains to humid conditions in the forest-covered Australian Alps, resulting in strong climatic variations. Where the topography allows, land use is mostly agricultural, ranging from extensive pastoral use to high-intensity agriculture applying irrigation along the mid and lower Murrumbidgee River. The *in situ* probes measure soil moisture at a depth of 5, 0–30, 30–60, and 60–90 cm [18]. Validation metrics are separately computed for the western and eastern clusters of *in situ* stations (see Fig. 1) and then averaged. Accompanying average confidence intervals for the correlations is computed per cluster and rescaled by the square-root of the number of clusters (here 2). As in [6], individual CI values are fully corrected for the large temporal autocorrelation of the hourly model output, and measurement errors at the individual *in situ* sites are assumed to be fully correlated within one cluster. CI values are thus considered to be very conservative estimates, and an increased number of independent clusters, e.g., within a global study, would result in smaller confidence intervals. The

TABLE I

CORRELATION R AND ANOMALY CORRELATION RA FOR SURFACE AND ROOT-ZONE (.RZ) SOIL MOISTURE AT THE OZNET SITES; 95% CONFIDENCE INTERVALS ARE SHOWN WITHIN BRACKETS

	R	Ra	R.rz	Ra.rz
OL	.70 (.37-.88)	.50 (.24-.70)	.47 (-.35-.91)	.52 (-.36-.91)
SMAPDA	.73 (.53-.85)	.63 (.42-.77)	.52 (-.20-.93)	.57 (-.17-.91)
SMOSDA	.73 (.53-.86)	.64 (.44-.78)	.52 (-.18-.94)	.57 (-.18-.92)
SMAPDA.s	.75 (.57-.87)	.64 (.45-.78)	.51 (-.16-.93)	.56 (-.17-.92)
SMOSDA.s	.74 (.54-.86)	.65 (.45-.79)	.52 (-.17-.95)	.57 (-.17-.92)
SMAPDA.x	.74 (.55-.86)	.65 (.46-.78)	.52 (-.18-.93)	.57 (-.15-.92)
SMOSDA.x	.74 (.54-.86)	.64 (.45-.78)	.51 (-.18-.95)	.56 (-.17-.91)

summary of the assimilation impact on correlations is shown in Table I with confidence intervals for the 95% confidence level added in brackets. The results are discussed in more detail in the following, including the mean impact on the root-mean-square error (RMSE).

A. Surface Soil Moisture

The two top CLM soil layers reach to a depth of approximately 5 cm, which roughly corresponds to the depth where the emitted L-band radiance is affected by soil moisture. Making use of the layer thickness, the weighted average of the modeled soil moisture is computed and compared with the OzNet*in situ* measurements taken at 5-cm depth, thereby excluding sites with less than 18 months of data. The average Pearson correlation coefficient R for the OL run is 0.70. Both the SMAPDA and SMOSDA experiments show a slightly increased R of 0.73. Larger improvements are visible when computing the correlation (Ra) between *in situ* soil moisture anomalies and modeled soil moisture anomalies. These anomalies are obtained by removing the respective soil moisture climatologies from the *in situ* and modeled time series. For the computation of the climatologies, a 31-day moving average across data from 2 years (from July 2015 to June 2017) is used, which corresponds to the method applied to create the Tb climatologies for experiments SMOSDA.s and SMAPDA.s as well as SMOSDA.x and SMAPDA.x. This allows to better assess the impact of assimilation, since the assimilation-induced changes in soil moisture otherwise are potentially masked by the large seasonal soil moisture gradient. Here, Ra increases from 0.50 for the OL run to 0.63 and 0.64 for SMAPDA and SMOSDA, respectively. For the experiments SMAPDA.s and SMOSDA.s, R increases to 0.75 and 0.74. The corresponding anomaly correlation Ra increases to 0.64 and 0.65. For the experiments using the cross-climatology SMAPDA.x and SMOSDA.x, R increases to 0.74 in both the cases. The anomaly correlation Ra increases to 0.65 and 0.64. The assimilation impacts on surface soil moisture anomalies at all *in situ* sites are shown in Fig. 2. It can be seen that especially the four experiments using a Tb climatology closely matching the assimilation period perform very similarly. For the RMSE between the simulated soil moisture and the *in situ* measurements (bias incl.), no impact is visible for any of the experiments and it remains at 0.05 m^3/m^3 (not shown). This is due to the fact that both the forecast and analysis time steps are included in validation, which hides the positive impact at the analysis time steps. Fig. 1 shows the assimilation impact on surface soil moisture anomalies for the experiments using SMAP observations. Similar to the overall statistics, also the spatial patterns are very similar between the experiments with some small differences. Assimilation has the largest impact on the *in situ* stations located in the more eastern part of the catchment (+0.2 and above). In the western cluster, improvements are lower (around +0.1) with a negative assimilation impact on a limited number of stations. For the experiment SMAPDA, the impact is slightly reduced at the western sites when compared with the SMAPDA.s and the SMAPDA.x. These findings closely match the experiments using SMOS observations (not shown here), where spatial patterns are equally similar to each other and to the experiments using SMAP observations. No obvious relationship between the described assimilation impact and the surrounding land cover of the *in situ* measurement sites could be identified.

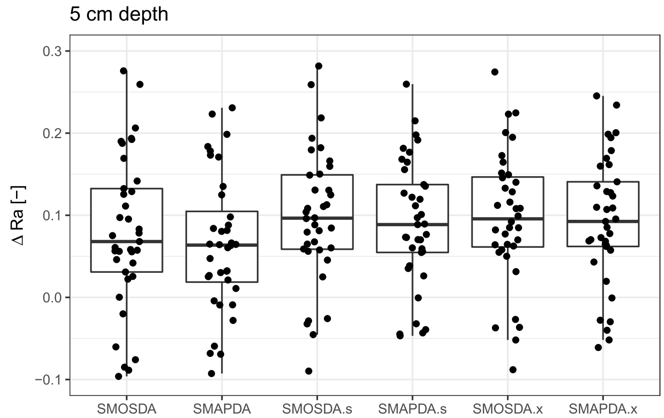

Fig. 2. Spatial distribution (boxplots) of the changes in Ra (ΔRa) between the modeled and the observed surface soil moisture for the OzNet *in situ* stations. ΔRa equals Ra after assimilation minus Ra for the OL. The horizontal lines correspond to the 75%, 50%, and 25% quantiles.

B. Root-Zone Soil Moisture

For the root-zone soil moisture (rz), *in situ* measurements are available at multiple depths, namely 0–30, 30-60, and 60–90 cm. As for surface soil moisture, the weighted average of the appropriate CLM layers is computed to allow for the comparison between the modeled and the measured soil moisture. OL performance R.rz is 0.47 and increases to 0.52 for both SMAPDA and SMOSDA and to 0.51 and 0.52 for SMAPDA.s and SMOSDA.s, respectively. Using the cross-climatology yields similar improvements with R 0.52 and 0.51 for SMAPDA.x and SMOSDA.x, respectively. For the RMSE, a slight reduction from 0.012 to 0.010 m^3/m^3 is achieved for all the experiments. Anomaly correlations Ra.rz increase from 0.52 for the OL to 0.56–0.57. It is to be noted that the impact of the experiments, including surface soil moisture, is not significant at the 95% CI level. This can be explained through the conservative estimation of the CI, accounting for the large temporal autocorrelation especially for the root zone, as mentioned above.

IV. Conclusion

The separate assimilation of SMOS and SMAP Tb anomalies has been carried out for April 2015–August 2017 across the Murrumbidgee basin and validated against *in situ* measurements from the OzNet network. For both the SMOS and the SMAP, assimilation was performed by using: 1) the long-term SMOS climatology using 7 years of data; 2) the climatology of the same sensor as the assimilated observations based on roughly the same time period as the observations, i.e., 2 full years; and 3) the same experiment as 2) but using the climatology of the other sensor. Assimilating the anomalies, in contrast to assimilating the original observations, was chosen to resolve for the seasonally differing Tb observation-minus-forecast bias. Together with the cdf-matching of the observation anomalies to the forward simulation anomalies, this avoided the need for calibrating the radiative transfer model CMEM and the possibility of reducing the sensitivity of the forward simulations to the changes in soil moisture. Improvements in R for surface soil moisture simulations are between 0.03 and 0.05 and when considering soil moisture anomalies R that increase by 0.13–0.15. This might highlight that the large seasonal gradient of soil moisture partly obscures the effect of the mostly quite small soil moisture increments. Improvements in R for the root zone are between 0.04 and 0.05 with similar differences in R when considering soil moisture anomalies. A slight reduction in the RMSE was achieved for the root zone. The main outcome of the study is that the SMOS and SMAP Tb data sets perform very similarly in estimating the soil moisture profile and that their respective longer and shorter term climatologies serve equally well in dealing with observation-minus-forecast biases. However, this insight might vary with the study region and different assimilation methods. Although it might have been expected that the SMAP Tb anomaly data assimilation would outperform the assimilation of SMOS Tb anomalies due to the higher radiometric accuracy and the larger data coverage (in time and space, due to the wider alias-free swath width, and the improved RFI mitigation for SMAP), the results do not support this. This is partly because all 30-min forecast and analysis time steps are included in the validation and because the assimilation design is not necessarily optimized for each experiment, e.g., in terms of (normalized) innovation statistics. Finally, RFI is not an issue within this specific study area. This letter demonstrates the usefulness of the available L-band data and its compatibility within a common assimilation system. Optimizing the use of both the data sources together should be the topic of future research.

Acknowledgment

The authors would like to thank R. Reichle for his contribution in developing the SMOS Level 1 Tb data corrected for both atmospheric contributions and galactic noise. *In situ* data from the OzNet measurement network were provided by the team at Monash University. The data assimilation system was downloaded from https://github.com/daspy/daspy and adapted for this study. The LETKF code coupled to the assimilation system was developed by T. Miyoshi (https://github.com/takemasa-miyoshi/letkf).

References

[1] D. Entekhabi, I. Rodriguez-Iturbe, and F. Castelli, "Mutual interaction of soil moisture state and atmospheric processes," *J. Hydrol.*, vol. 184, nos. 1–2, pp. 3–17, 1996. [Online]. Available: http://www.sciencedirect.com/science/article/pii/0022169495029656

[2] E. G. Njoku and J.-A. Kong, "Theory for passive microwave remote sensing of near-surface soil moisture," *J. Geophys. Res.*, vol. 82, no. 20, pp. 3108–3118, 1977, doi: 10.1029/JB082i020p03108.

[3] Y. H. Kerr, P. Waldteufel, J.-P. Wigneron, J. Martinuzzi, J. Font, and M. Berger, "Soil moisture retrieval from space: The Soil Moisture and Ocean Salinity (SMOS) mission," *IEEE Trans. Geosci. Remote Sens.*, vol. 39, no. 8, pp. 1729–1735, Aug. 2001.

[4] D. Entekhabi *et al.*, "The Soil Moisture Active Passive (SMAP) mission," *Proc. IEEE*, vol. 98, no. 5, pp. 704–716, May 2010.

[5] S. V. Kumar, R. H. Reichle, R. D. Koster, W. T. Crow, and C. D. Peters-Lidard, "Role of subsurface physics in the assimilation of surface soil moisture observations," *J. Hydrometeorol.*, vol. 10, no. 6, pp. 1534–1547, Dec. 2009.

[6] G. J. M. De Lannoy and R. H. Reichle, "Global assimilation of multi-angle and multipolarization SMOS brightness temperature observations into the GEOS-5 catchment land surface model for soil moisture estimation," *J. Hydrometeorol.*, vol. 17, no. 2, pp. 669–691, 2016, doi: 10.1175/JHM-D-15-0037.1.

[7] S. Chan E. G. Njoku, and A. Colliander, "SMAP L1C radiometer half-orbit 36 km EASE-grid brightness temperatures, version 3," NASA Nat. Snow Ice Data Center Distrib. Act. Arch. Center, Boulder, CO, USA, Tech. Rep., 2016. [Online]. Available: http://nsidc.org/data/SPL1CTB/versions/3

[8] R. H. Reichle *et al.*, "Global assessment of the SMAP Level-4 surface and root-zone soil moisture product using assimilation diagnostics," *J. Hydrometeorol.*, vol. 18, no. 12, pp. 3217–3237, 2017.

[9] H. Lievens *et al.*, "Assimilation of SMOS soil moisture and brightness temperature products into a land surface model," *Remote Sens. Environ.*, vol. 180, pp. 292–304, Jul. 2016.

[10] D. Rains, X. Han, H. Lievens, C. Montzka, and N. Verhoest, "SMOS brightness temperature assimilation into the community land model," *Hydrol. Earth Syst. Sci.*, vol. 21, no. 11, pp. 5929–5951, 2017. [Online]. Available: https://www.hydrol-earth-syst-sci.net/21/5929/2017/

[11] K. W. Oleson *et al.*, "Technical description of version 4.0 of the Community Land Model (CLM)," Nat. Center Atmos. Res., Boulder, CO, USA, Tech. Rep. NCAR/TN-478+STR, 2013. [Online]. Available: http://citeseerx.ist.psu.edu/viewdoc/download?doi=10.1.1.172.7769&rep=rep1&type=pdfs

[12] D. P. Dee *et al.*, "The ERA-Interim reanalysis: Configuration and performance of the data assimilation system," *Quart. J. Roy. Meteorol. Soc.*, vol. 137, pp. 553–597, Apr. 2011.

[13] J. M. Sabater, P. de Rosnay, C. Albergel, and L. Isaksen, "Sensitivity of soil moisture analyses to contrasting background and observation error scenarios," in *Proc. EGU Gen. Assembly Conf. Abstr.*, 2017, p. 19199.

[14] H. Lievens, B. Martens, N. E. C. Verhoest, S. Hahn, R. H. Reichle, and D. G. Miralles, "Assimilation of global radar backscatter and radiometer brightness temperature observations to improve soil moisture and land evaporation estimates," *Remote Sens. Environ.*, vol. 189, pp. 194–210, Feb. 2017. [Online]. Available: http://www.sciencedirect.com/science/article/pii/S0034425716304709

[15] G. J. M. De Lannoy *et al.*, "Converting between SMOS and SMAP level-1 brightness temperature observations over nonfrozen land," *IEEE Geosci. Remote Sens. Lett.*, vol. 12, no. 9, pp. 1908–1912, Sep. 2015.

[16] B. R. Hunt, E. J. Kostelich, and I. Szunyogh, "Efficient data assimilation for spatiotemporal chaos: A local ensemble transform Kalman filter," *Phys. D, Nonlinear Phenom.*, vol. 230, nos. 1–2, pp. 112–126, 2007. [Online]. Available: http://www.sciencedirect.com/science/article/pii/S0167278906004647

[17] G. Gaspari and S. E. Cohn, "Construction of correlation functions in two and three dimensions," *Quart. J. Roy. Meteorol. Soc.*, vol. 125, no. 554, pp. 723–757, 1999.

[18] A. Smith *et al.*, "The Murrumbidgee soil moisture monitoring network data set," *Water Resour. Res.*, vol. 48, no. 7, p. W07701, 2012.